

Competition of Thermodynamic and Kinetic Factors during the Formation of Stereoisomers of the Bis(chelate) Ni(II) Complexes Based on (N,O(S,Se))-Bidentate Azomethines: A Quantum Chemical Study

N. N. Kharabayev^a, * and V. I. Minkin^a

^a Institute of Physical and Organic Chemistry, Southern Federal University, Rostov-on-Don, Russia

*e-mail: nkhgarabaev@mail.ru

Received July 6, 2022; revised August 25, 2022; accepted August 26, 2022

Abstract—The molecular structures and relative energies of *trans*- and *cis*-isomers of low-spin bis(chelate) Ni(II) complexes based on (N,O(S,Se))-bidentate azomethines are calculated by the density functional theory. The mechanism of formation of the NiL₂ complexes is studied in terms of the model of their step formation (Ni⁺⁺ + (L)⁻ → (NiL)⁺, (NiL)⁺ + (L)⁻ → NiL₂). The formation of the coordination sites NiN₂O₂, NiN₂S₂, and NiN₂Se₂ of the complexes is determined by the energy preference of one of possible configurations and also by the activation barriers of isomerization of the primary products formed at the initial step of the reaction of the starting components.

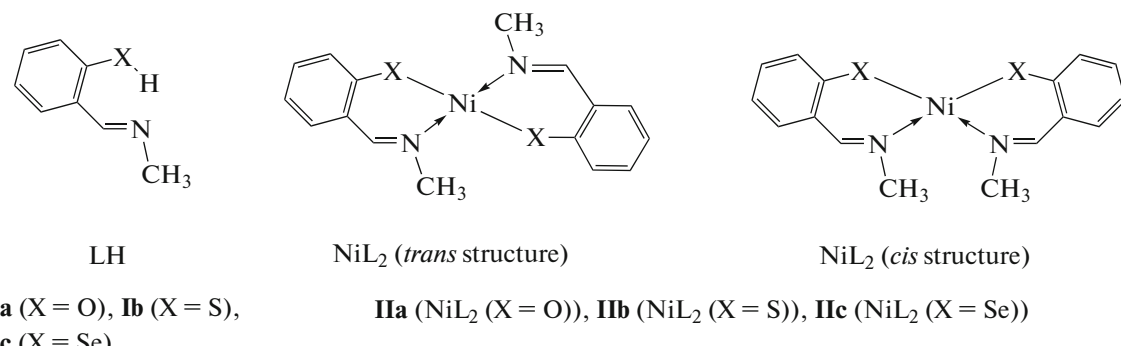
Keywords: quantum chemical modeling, bis(chelate) nickel complexes, stereoisomerization, azomethines

DOI: 10.1134/S1070328422700117

INTRODUCTION

The molecular structures and spectral, magnetic, and other physicochemical properties of bis(chelate) complexes of 3d-transition metals with azomethine ligands are mainly predetermined by the composition and configuration of the MN_2X_2 coordination site ($X = O, S, Se$) and structural features of the ligands. These regularities were experimentally [1–3] and theoretically [4–6] studied in most detail for the bis(chelate) Ni(II) complexes based on (N,O)-, (N,S)-, and (N,Se)-bidentate azomethines in which the central ion can take *trans*-planar, *cis*-planar, or pseudotetra-

hedral configurations. The azomethine NiL_2 complexes with the NiN_2O_2 coordination site are characterized by the trans structure [1, 7–11], whereas the cis structure is characteristic of the complexes with the NiN_2S_2 and NiN_2Se_2 coordination sites [1, 12–16]. For the theoretical interpretation of this stereoeffect, we performed the quantum chemical study of the relative stability and reaction routes of formation of the *trans*- and *cis*-planar isomers depending on the composition of the nearest environment of the central ion in low-spin bis(chelate) azomethine nickel complexes **IIa** (NiL_2 ($\text{X} = \text{O}$)), **IIb** (NiL_2 ($\text{X} = \text{S}$)), and **IIc** (NiL_2 ($\text{X} = \text{Se}$)).



A theoretical search for the most preferred *trans*- or *cis*-planar stereoisomers was performed using the earlier proposed approach [17] based on the determination of the energetically most favorable stereoisomer using the density functional theory (DFT) calculations and evaluation of the accessibility (probability of formation) of this stereoisomer during complex formation applying the step model of the reaction mechanism of formation of metal complexes ML_2



The second step of this reaction (coupling by the cation $(ML)^+$ of the anion of the second ligand $(L)^-$) is the main stage for the determination of the isomer most probable in complex formation. If the kinetically most accessible stereoisomer also represents its energetically preferred form, then this isomer can be predicted as the expected product of reaction (1). In the opposite case, this isomer would be considered as the initial one for possible subsequent isomerization reactions directed toward more stable isomeric structures, which requires an additional estimation of the energy barriers of the corresponding stereoisomerization reactions.

CALCULATION PROCEDURE

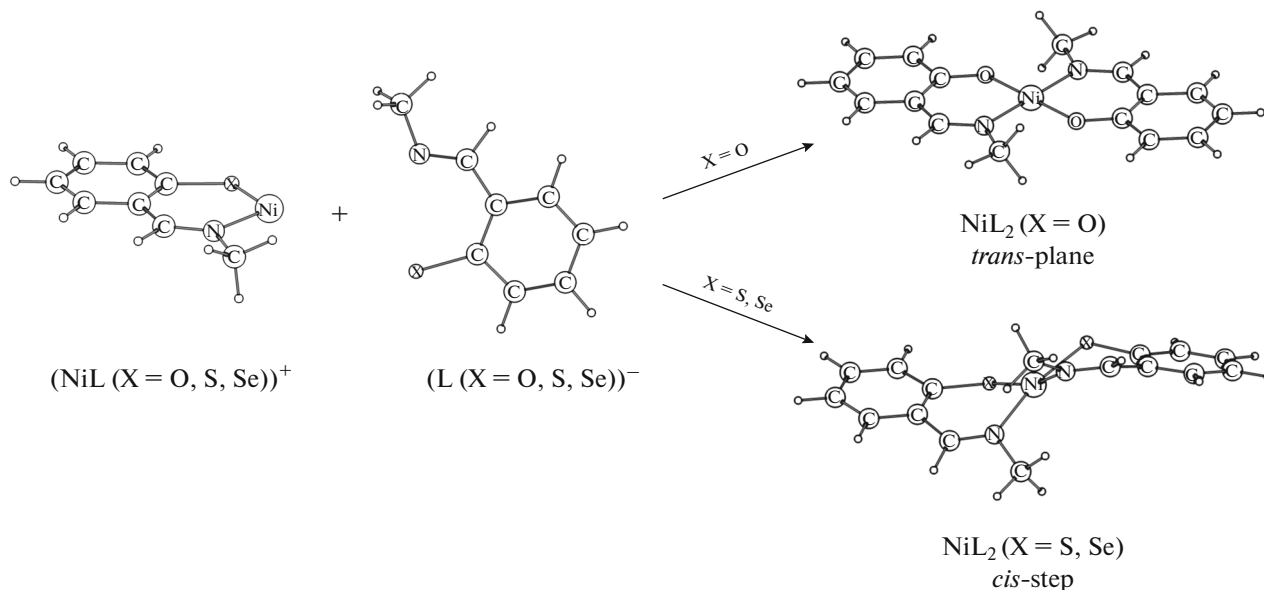
Quantum chemical calculations were performed by the DFT method [18] using the Gaussian09 program [19]. Since DFT calculation results are known to depend on the type of the functional used [20–22], the calculations were performed using three variants of hybrid functionals: B3LYP [23, 24], PBE0 [25], and TPSSh [26] combined with the 6-311++G(d,p) basis set. The low-spin (singlet) state was taken into account in the calculations of the *trans*- and *cis*-stereoisomers of the Ni(II) complexes. Stationary points on the

potential energy surface (PES) were localized and analyzed by the full geometry optimization of the stereoisomers of the Ni(II) complexes accompanied by the calculation of the vibrational spectra for the ground states of the stereoisomers and structures coupling their transition states. When studying spin-forbidden mechanisms of *cis*–*trans*-isomerization in the bis(chelate) Ni(II) complexes, the minimum energy crossing points (MECP) of the singlet and triplet PES were found by the Harvey procedure [27]. The graphical images of the molecular structures were constructed using the ChemCraft program [28].

RESULTS AND DISCUSSION

The quantum chemical modeling of the reaction $(NiL)^+ + (L)^- \rightarrow NiL_2$ (at the starting distance (equal to 5 Å) between the nickel atom of the $(NiL)^+$ cation and N and X (O, S, Se) donor atoms of the second ligand $(L)^-$, respectively, with allowance for the starting mutual orthogonal arrangement of planes of the $(NiL)^+$ cation from one side and the “claw” of the anion of the second ligand $(L)^-$ from another side) made it possible to determine the isomers kinetically most accessible during complex formation for each complex of considered nickel complexes **IIa** (X = O), **IIb** (X = S), and **IIc** (X = Se) presented in Scheme 1.

The model reaction $(ML)^+ + (L)^- \rightarrow ML_2$ of formation of the molecular structures (DFT/B3LYP/6-311++G(d,p)) of the NiL_2 bis(chelate) complexes (X = O, S, Se) is shown in Scheme 1. The product of this reaction for complex NiL_2 (X = O) is the *trans*-planar isomer, whereas the *cis*-isomer in the “step” conformation was determined for complexes NiL_2 (X = S) and NiL_2 (X = Se) (Scheme 1).



Scheme 1.

Table 1. Calculated relative energies ignoring (ΔE , kcal/mol) and taking into account zero-point vibrations (ΔE_{ZPE} , kcal/mol) for the stereoisomers of low-spin nickel complexes **IIa** ($X = O$), **IIb** ($X = S$), and **IIc** ($X = Se$)

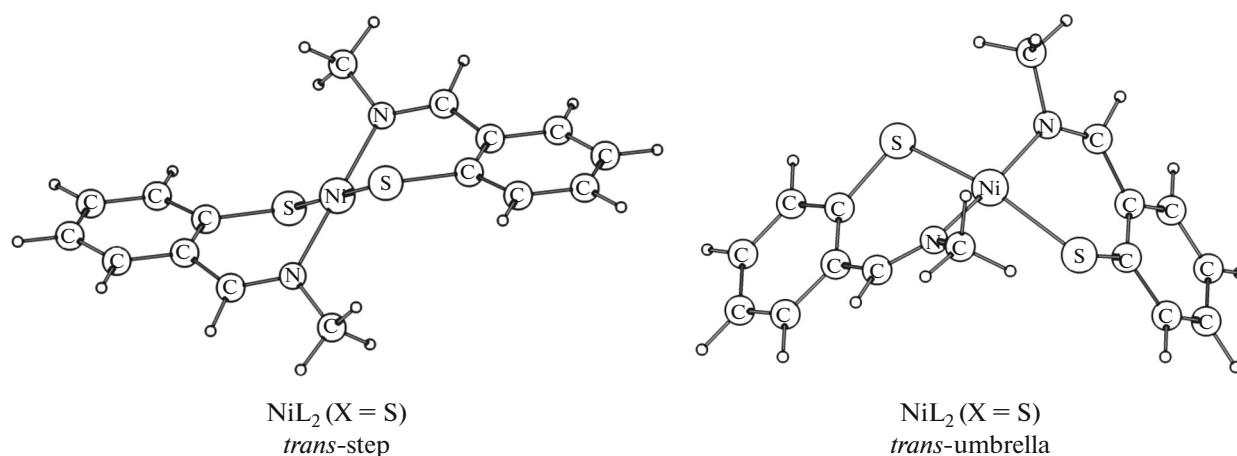
Stereoisomers of complexes NiL_2 ($X = O, S, Se$)	DFT/B3LYP		DFT/PBE0		DFT/TPSSh	
	ΔE	ΔE_{ZPE}	ΔE	ΔE_{ZPE}	ΔE	ΔE_{ZPE}
IIa ($X = O$), <i>trans</i> -plane*	0.0	0.0	0.0	0.0	0.0	0.0
IIa ($X = O$), <i>cis</i> -step	13.3	12.6	13.2	12.5	12.8	12.0
IIb ($X = S$), <i>trans</i> -umbrella	-1.6	-1.3	-1.7	-1.4	-1.1	-0.9
IIb ($X = S$), <i>trans</i> -step	1.4	1.5	1.1	1.2	1.7	1.7
IIb ($X = S$), <i>cis</i> -step*	0.0	0.0	0.0	0.0	0.0	0.0
IIc ($X = Se$), <i>trans</i> -umbrella	0.3	0.5	0.3	0.6	1.1	1.3
IIc ($X = Se$), <i>trans</i> -step	2.9	3.2	2.5	2.7	3.3	3.6
IIc ($X = Se$), <i>cis</i> -step*	0.0	0.0	0.0	0.0	0.0	0.0

* The most kinetically accessible isomer for complex formation (Scheme 1).

The obtained result was interpreted by a step-by-step analysis of the reaction $(NiL)^+ + (L)^- \rightarrow NiL_2$ for each complex of nickel complexes **IIa** ($X = O$), **IIb** ($X = S$), and **IIc** ($X = Se$). The analysis showed that the coupling by the $(NiL)^+$ cation of the anion of the second (L^-) ligand led to the formation of the bond of the Ni atom first with the X atom and then with the N atom of the second ligand accompanied by flattening of the coordination site NiN_2X_2 ($X = O, S, Se$), which is characteristic of the low-spin nickel(II) complexes. The preferred direction of motion of the X atom of the second ligand toward either X atom, or N atom of the $(NiL)^+$ cation, which predetermines the formation of either *cis*, or *trans* structure of the complex, is chosen according to the ratio of electronegativities of X atoms ($X = O, S, Se$) and N atom. For O-containing complex **IIa**, the motion of the O atom of the second ligand toward the N atom is preferred rather the O atom of the first ligand (*trans* structure is the result). For S- and Se-containing complexes **IIb** and **IIc**, respectively, the motion of the S (Se) atom of the second ligand toward the S (Se) atom is preferred rather than the N atom of the first ligand (*cis* structure is the

result). Thus, the *trans*-isomer of nickel complex **IIa** ($X = O$) and *cis*-isomers of nickel complexes **IIb** ($X = S$) and **IIc** ($X = Se$) kinetically most accessible in complex formation are formed in terms of the proposed model, which is shown in Scheme 1.

The most favorable (by total energy) stereoisomers for each complex of the considered nickel complexes are determined by the relative energies of the competing *trans*- and *cis*-isomers of low-spin complexes **IIa**, **IIb**, and **IIc** (Table 1). The energies of the competing stereoisomers were determined relative to the isomer kinetically most accessible in complex formation, i.e., initial for the possible subsequent transformation. The planar *trans*-isomer is energetically most favorable for complex **IIa** ($X = O$) (Scheme 1), the *trans*-isomer in the “umbrella” conformation is most favorable for complex **IIb** ($X = S$), and the *cis*-isomer in the “step” conformation is energetically most favorable for complex **IIc** ($X = Se$) (Scheme 1). The calculated (DFT/B3LYP/6-311++G(d,p)) molecular structures of the “*trans*-step” and “*trans*-umbrella” conformers for complex NiL_2 ($X = S$) are shown in Scheme 2.



Scheme 2.

Table 2. Calculated (DFT/B3LYP/6-311++G(d,p)) geometric parameters of the coordination sites NiN_2X_2 in the *trans*- and *cis*-isomers of the NiL_2 complexes ($\text{X} = \text{O}, \text{S}, \text{Se}$), transition states (TS) of *cis*–*trans*-isomerization, and MECP 1 and MECP 2 points

Stereoisomers of complexes NiL_2 ($\text{X} = \text{O}, \text{S}, \text{Se}$)	$\text{Ni}-\text{X}$, Å	$\text{Ni}-\text{N}$, Å	$\angle \text{NNiX}$, deg	$\angle \text{XNiX}$, deg	$\angle \text{NNiN}$, deg	α , deg	β , deg
IIa ($\text{X} = \text{O}$), <i>trans</i> -step	1.855	1.943	92.8	179.9	179.9	130.9	0.0
IIa ($\text{X} = \text{O}$), <i>cis</i> -step	1.869	1.917	91.7	85.0	94.9	125.7	25.7
TS (IIa , “ <i>trans</i> -plane → → <i>cis</i> -step”)*	1.823	1.853	95.9	123.0	111.1	128.5	3.0
MECP 1 (IIa , $\text{X} = \text{O}$)	1.905	1.966	92.2	150.5	167.3	124.3	24.6
MECP 2 (IIa , $\text{X} = \text{O}$)	1.898	1.945	92.6	91.6	97.5	127.3	16.3
IIb ($\text{X} = \text{S}$), <i>trans</i> -umbrella	2.246	1.930	91.3	163.7	170.4	105.0	39.8
IIb ($\text{X} = \text{S}$), <i>trans</i> -step	2.254	1.944	88.2	180.0	180.0	102.4	49.8
IIb ($\text{X} = \text{S}$), <i>cis</i> -step	2.207	1.957	91.9	85.7	93.2	105.5	37.6
TS (IIb , “ <i>cis</i> -step → → <i>trans</i> -umbrella”)*	2.165	1.872	96.7	112.1	124.4	111.3	10.0
MECP 1 (IIb , $\text{X} = \text{S}$)	2.219	1.980	96.1	92.6	97.2	110.2	14.1
MECP 2 (IIb , $\text{X} = \text{S}$)	2.264	2.000	94.0	143.4	164.0	107.6	31.0
IIc ($\text{X} = \text{Se}$), <i>trans</i> -umbrella	2.371	1.926	90.6	162.7	170.8	99.3	44.3
IIc ($\text{X} = \text{Se}$), <i>trans</i> -step	2.386	1.937	87.0	180.0	180.0	95.5	55.7
IIc ($\text{X} = \text{Se}$), <i>cis</i> -step	2.319	1.966	91.4	86.1	93.4	100.5	41.1
TS (IIc , “ <i>cis</i> -step → → <i>trans</i> -umbrella”)*	2.290	1.875	96.8	110.4	127.2	107.6	7.0
MECP 1 (IIc , $\text{X} = \text{Se}$)	2.333	1.988	96.0	94.0	96.3	106.0	17.5
MECP 2 (IIc , $\text{X} = \text{Se}$)	2.385	2.008	93.3	142.4	162.5	101.8	36.0

* The double geometric parameters of the metallocycles in the TS of *cis*–*trans*-isomerization in complexes **IIb** ($\text{X} = \text{S}$) and **IIc** ($\text{X} = \text{Se}$) show nonequivalence of the metallocycle structures.

Scheme 2 shows the molecular structures of the *trans*-isomers of S-containing nickel complex **IIb** in the “step” and “umbrella” conformations, which are (according to the total energy (Table 1)) competitive with respect to the *cis*-isomer in the “step” conformation, which is kinetically most accessible in the formation of this complex (Scheme 1). The calculated structures of analogous isomers of S-containing complex **IIc** visually nearly coincide with the structures presented in Scheme 2. The geometric parameters of the NiN_2X_2 coordination sites ($\text{X} = \text{O}, \text{S}, \text{Se}$) in the calculated molecular structures of the *trans*- and *cis*-isomers of nickel complexes **IIa**, **IIb**, and **IIc** are given in Table 2.

For O-containing nickel complex **IIa**, the *cis* structure of the complex, which is competitive toward the planar *trans*-isomer (Scheme 1), is sterically hindered because of interligand interactions of the substituents at the azomethine nitrogen atoms. As compared to O-containing nickel complex **IIa**, the *cis* structure of the complex (along with the *trans* structure) is sterically accessible for S- and Se-containing complexes **IIb** and **IIc** (Scheme 1) due to considerable inflections (by angle β) of the metallocycle along the

S–N or Se–N lines (Table 2). As mentioned previously [29], these inflections of the metallocycles are related to small bond (intracyclic) angles α (Table 2) characteristic of sulfur and selenium atoms (unlike oxygen atoms).

In the case of O-containing nickel complex **IIa**, the *trans*-planar isomer kinetically most accessible for complex formation, i.e., product of model reaction (1) shown in Scheme 1, is also energetically preferred (Table 1) over the *cis*-isomer by 12 kcal/mol (Table 1), which predetermines a high barrier for stereoisomerization from the initial *trans*-isomer to the competing *cis*-isomer (according to the DFT/B3LYP/6-311++G(d,p) calculation, the barrier of this reaction is 39.3 kcal/mol).

The use of the alternative model of the stereoisomerization mechanism [30] that takes into account a possible (in the bis(chelate) azomethine Ni(II) complexes) intersection of the singlet and triplet PES also suggests a high barrier of the interconfigurational transition in nickel complex **IIa** ($\text{X} = \text{O}$) from the kinetically most accessible *trans*-isomer to the competing *cis*-isomer. In terms of this model, the *trans*–*cis*-isomerization of nickel complex **IIa** ($\text{X} = \text{O}$) can be pre-

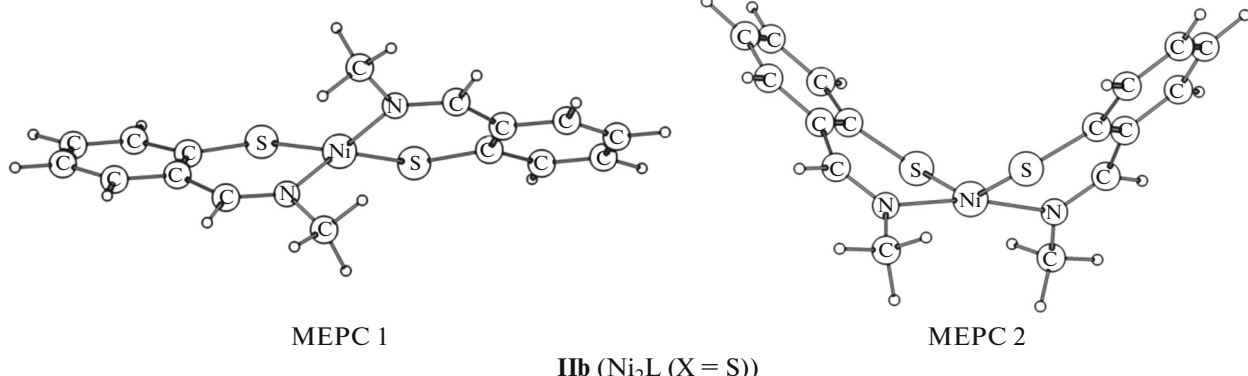
sented as two consecutive spin-forbidden transitions “*trans*-planar isomer (singlet) → pseudotetrahedron (triplet)” and “pseudotetrahedron (triplet) → *cis*-isomer in step conformation (singlet).” To estimate the barriers of these spin-forbidden transitions, the molecular structures of nickel complex **IIa** ($X = O$) at the minimum (in energy) points of intersection of the singlet and triplet PES were calculated by the Harvey procedure [27]. The MECP 1 and MECP 2 points (Table 2) characterize, correspondingly, the first and second transitions of two consecutive spin-forbidden transitions in nickel complex **IIa** ($X = O$). According to the DFT/B3LYP/6-311++G(d,p) calculations, the MECP 1 point (transition “*trans*-planar isomer → pseudotetrahedron”) is remote (by total energy) from the local minimum of nickel complex **IIa** ($X = O$) in the starting *trans*-planar configuration by 9.4 kcal/mol, whereas the MECP 2 point (transition “pseudotetrahedron → *cis*-step”) is remote from the local minimum of the complex on the triplet PES (configuration “pseudotetrahedron”) by 13.8 kcal/mol.

The high barrier of *trans*–*cis*-isomerization in nickel complex **IIa** ($X = O$), which was found in both the model of this reaction mechanism taking into account one singlet PES and the alternative model with allowance for two intersecting (singlet and triplet) PES, suggests the preference of the isomer initial in this reaction, i.e., kinetically most accessible for the complex formation of the *trans*-planar isomer as the product of the model reaction $(NiL)^+ + (L)^- \rightarrow NiL_2$ ($X = O$, Scheme 1).

Unlike O-containing nickel complex **IIa**, in the case of S-containing nickel complex **IIb**, the most kinetically accessible in complex formation *cis*-isomer in the “step” conformation (Scheme 1) is not the most stable form (Table 1). In addition, it is important that the competing *cis*- and *trans*-isomers of S-containing complex **IIb** differ in total energy by approximately 1 kcal/mol only (Table 1). Therefore, according to the step model of the mechanism of formation of the

bis(ligand) complexes [17], the most accessible in complex formation *cis*-isomer of complex **IIb** ($X = S$) in the “step” conformation (Scheme 1) is accepted only as the initial one for possible isomerization to the energetically more favorable *trans*-isomer in the “umbrella” conformation (Table 1) followed by the estimation of the *cis*–*trans*-isomerization barrier. According to the DFT calculation of the transition state of the “*cis*-step → *trans*-umbrella” isomerization (Table 2) determined by the simulation of this reaction mechanism in nickel complex **IIb** ($X = S$) on the singlet PES, including the starting and finishing isomers, the *cis*–*trans*-isomerization barrier exceeds 20 kcal/mol (24.3 (B3LYP), 26.8 (PBE0), and 25.1 (TPSSh) kcal/mol).

The conclusion about a high barrier of the interconfigurational transition in nickel complex **IIb** ($X = S$) from the kinetically most accessible *cis*-isomer in the “step” conformation (Scheme 1) to the energetically more favorable *trans*-isomer in the “umbrella” conformation (Table 1) also follows from the alternative model of the stereoisomerization mechanism [30] taking into account a possible intersection of the singlet and triplet PES. In terms of this model, the *cis*–*trans*-isomerization of nickel complex **IIb** ($X = S$) can be presented as two consecutive spin-forbidden transitions: “*cis*-step (singlet) → pseudotetrahedron (triplet)” and “pseudotetrahedron (triplet) → *trans*-umbrella (singlet).” According to the DFT calculations for nickel complex **IIb** ($X = S$), the MECP 1 point characterizing the spin-forbidden transition “*cis*-step → pseudotetrahedron” (Table 2, Scheme 3) is remote by total energy from the local minimum of the complex in the starting “*cis*-step” configuration by 4.3 (B3LYP), 4.1 (PBE0), and 6.2 (TPSSh) kcal/mol, and the MECP 2 point that characterizes the second transition of two consecutive spin-forbidden transitions (“pseudotetrahedron → *trans*-umbrella” (Table 2, Scheme 3)) is remote from the local minimum of the complex on the triplet PES by 8.2 (B3LYP), 9.5 (PBE0), and 6.0 (TPSSh) kcal/mol.



Scheme 3.

The high barrier of *cis*–*trans*-isomerization in nickel complex **IIb** (X = S), which was found in both the model of this reaction with allowance for one singlet PES and the alternative model taking into account two intersecting (singlet and triplet) PES, suggests the preference of the isomer initial in the reaction, i.e., the kinetically most accessible in complex formation *cis*-isomer in the “step” conformation as the product of the reaction $(\text{NiL})^+ + (\text{L})^- \rightarrow \text{NiL}_2$ (X = S, Scheme 1).

In the case of Se-containing nickel complex **IIc**, the kinetically most accessible in complex formation *cis*-isomer in the “step” conformation (Scheme 1) is also the energetically most favorable isomer (Table 1). However, it should be taken into account that, as in the case of S-containing complex **IIb**, the competing *cis*- and *trans*-isomers differ in total energy by ~1 kcal/mol only. Therefore, the kinetically most accessible in complex formation *cis*-isomer of nickel complex **IIc** (X = Se) in the “step” conformation (Scheme 1) can be accepted as the preferred one only if the barrier of the “*cis*-step \rightarrow *trans*-umbrella” isomerization is significant. The localization of the transition state for this reaction when modeling its mechanism on the singlet PES (Table 2) made it possible to estimate the energy barrier by a value close to that obtained for S-containing nickel complex **IIb**, i.e., higher than 20 kcal/mol (24.3 (B3LYP), 26.5 (PBE0), and 24.8 (TPSSh) kcal/mol).

The conclusion about a high barrier of the inter-configurational transition in nickel complex **IIc** (X = Se) from the kinetically most accessible *cis*-isomer in the “step” conformation (Scheme 1) to the competing *trans*-isomer in the “umbrella” conformation (Table 1) can also be drawn for the alternative model of stereoisomerization [30] taking into account a possible intersection of the singlet and triplet PES. In terms of this model, the *cis*–*trans*-isomerization of nickel complex **IIc** (X = Se) can be presented (as well as for complex **IIb** (X = S)) as two consecutive spin-forbidden transitions “*cis*-step (singlet) \rightarrow pseudotetrahedron (triplet)” and “pseudotetrahedron (triplet) \rightarrow *trans*-umbrella (singlet).” According to the DFT calculations for nickel complex **IIc** (X = Se), the MECP 1 point, which characterizes the spin-forbidden transition “*cis*-step \rightarrow pseudotetrahedron” (Table 2), is remote (by total energy) from the local minimum of the complex in the starting configuration “*cis*-step” by 4.8 (B3LYP), 4.7 (PBE0), and 6.5 (TPSSh) kcal/mol. The MECP 2 point characterizing the second one of two consecutive spin-forbidden transitions (“pseudotetrahedron \rightarrow *trans*-umbrella” (Table 2)) is remote, according to the calculations, from the local minimum of the complex on the triplet PES by 8.7 (B3LYP), 10.3 (PBE0), and 6.8 (TPSSh) kcal/mol. Note that the calculated molecular structures of nickel complex **IIc** (X = Se) at the MECP 1 and MECP 2 points visually do not differ from the

corresponding structures of nickel complex **IIb** (X = S) shown in Scheme 3.

Thus, the high barrier of the *cis*–*trans*-isomerization was found in nickel complexes **IIc** (X = Se) and **IIb** (X = S), which suggests that the isomer initial in this reaction, i.e., kinetically most accessible in the complex formation of the *cis*-isomer in the “step” conformation, is preferred as the product of the model reaction $(\text{NiL})^+ + (\text{L})^- \rightarrow \text{NiL}_2$ (X = Se, Scheme 1).

The conclusions made in terms of theoretical analysis about the preferred *trans*-planar isomer for O-containing nickel complex **IIa** (X = O) and *cis*-isomer in the “step” conformation for S- and Se-containing nickel complexes **IIb** (X = S) and **IIc** (X = Se), respectively, are consistent with the experimental results [1, 7–16].

To conclude, as follows from the study performed, the preferred stereoisomer corresponds to the product of the reaction $(\text{NiL})^+ + (\text{L})^- \rightarrow \text{NiL}_2$ (X = O, S, Se, Scheme 1) for all considered O-, S-, and Se-containing low-spin azomethine nickel complexes **IIa**, **IIb**, and **IIc**. The simulation of this reaction for nickel complexes **IIa** (X = O), **IIb** (X = S), and **IIc** (X = Se) made it possible to reproduce the regularity of formation of the *trans* structure of the NiN_2O_2 coordination site and *cis* structure of the NiN_2S_2 and NiN_2Se_2 coordination sites, which was experimentally documented for the low-spin azomethine nickel(II) complexes. Therefore, structure formation of the NiN_2O_2 , NiN_2S_2 , and NiN_2Se_2 coordination sites of the low-spin bis(chelate) azomethine nickel(II) complexes is predetermined by the kinetics of the isomerization reactions on which the method is based (activation barriers of isomerization of the primary products formed in the initial step of interactions of the starting components) rather than by the thermodynamic factors (energy preference of one of possible conformations).

FUNDING

This work was supported by the Ministry of Science and Higher Education of the Russian Federation (state assignment in the field of scientific activity, project no. 0852-2020-0031).

CONFLICT OF INTEREST

The authors declare that they have no conflicts of interest.

REFERENCES

1. Garnovskii, A.D., Nivorozhkin, A.L., and Minkin, V.I., *Coord. Chem. Rev.*, 1993, vol. 126, no. 1, p. 1.
2. Bourget-Merle, L., Lappert, M.F., and Severn, J.R., *Chem. Rev.*, 2002, vol. 102, no. 6, p. 3031.

3. Garnovskii, A.D., Vasilchenko, I.S., Garnovskii, D.A., and Kharisov, B.I., *J. Coord. Chem.*, 2009, vol. 62, no. 2, p. 151.
4. Kharabaev, N.N., Starikov, A.G., and Minkin, V.I., *Dokl. Chem.*, 2014, vol. 458, p. 181.
5. Kharabayev, N.N., Starikov, A.G., and Minkin, V.I., *Russ. J. Coord. Chem.*, 2015, vol. 41, no. 7, p. 421. <https://doi.org/10.1134/S1070328415070039>
6. Kharabayev, N.N., Starikov, A.G., and Minkin, V.I., *J. Struct. Chem.*, 2016, vol. 57, no. 3, p. 431.
7. Lacroix, P.G., Averseng, F., Malfant, I., and Nakatani, K., *Inorg. Chim. Acta*, 2004, vol. 357, p. 3825.
8. Song, X., Wang, Z., Zhao, J., and Hor, T.S.A., *Chem. Commun.*, 2013, vol. 49, p. 4992.
9. Chen, L., Zhong, Z., Chen, C., et al., *J. Organomet. Chem.*, 2014, vol. 752, p. 100.
10. Chandrakala, M., Bharath, S., Maiyalagan, T., and Arockiasamy, S., *Mater. Chem. Phys.*, 2017, vol. 201, p. 344.
11. Conejo, M., Cantero, J., Pastor, A., et al., *Inorg. Chim. Acta*, 2018, vol. 470, p. 113.
12. Nivorozhkin, A.L., Nivorozhkin, L.E., Minkin, V.I., et al., *Polyhedron*, 1991, vol. 10, p. 179.
13. Mistryukov, A.E., Vasil'chenko, I.S., Sergienko, V.S., et al., *Mendeleev Commun.*, 1992, vol. 2, no. 1, p. 30.
14. Fierro, C.M., Murphy, B.P., Smith, P.D., et al., *Inorg. Chim. Acta*, 2006, vol. 359, p. 2321.
15. Orysyk, S.I., Bon, V.V., Pekhnyo, V.I., et al., *Polyhedron*, 2012, vol. 38, p. 15.
16. Bredenkamp, A., Zenq, X., and Mohr, F., *Polyhedron*, 2012, vol. 33, p. 107.
17. Kharabayev, N.N., *Russ. J. Coord. Chem.*, 2019, vol. 45, no. 8, p. 673. <https://doi.org/10.1134/S1070328419080050>
18. Parr, R. and Yang, W., *Density-Functional Theory of Atoms and Molecules*, New York: Oxford University, 1989.
19. Frisch, M.J., Trucks, G.W., Schlegel, H.B., et al., *Gaussian 09. Revision D.01*, Wallingford CT: Gaussian, 2013.
20. Sousa, S.F., Fernandes, P.A., and Ramos, M.J., *J. Phys. Chem. A*, 2007, vol. 111, no. 42, p. 10439.
21. Burke, K. and Wagner, L.O., *Int. J. Quantum Chem.*, 2013, vol. 113, no. 2, p. 96.
22. Tsipis, A.C., *Coord. Chem. Rev.*, 2014, vol. 272, p. 1.
23. Becke, A.D., *Phys. Rev. A: At., Mol. Opt., Phys.*, 1988, vol. 38, p. 3098.
24. Lee, C., Yang, W., and Parr, R.G., *Phys. Rev. B*, 1988, vol. 37, p. 785.
25. Perdew, J.P., Burke, K., and Ernzerhof, M., *Phys. Rev. Lett.*, 1996, vol. 77, p. 3865.
26. Tao, J., Perdew, J.P., Staroverov, V.N., and Scuseria, G.E., *Phys. Rev. Lett.*, 2003, vol. 91, p. 146401.
27. Harvey, J.N., Aschi, M., Schwarz, H., and Koch, W., *Theor. Chem. Acc.*, 1998, vol. 99, no. 2, p. 95.
28. Zhurko, G.A. and Zhurko, D.A., *Chemcraft Version 1.6*, URL: <http://www.chemcraftprog.com>.
29. Kharabaev, N.N., *Koord. Khim.*, 1991, vol. 17, no. 5, p. 579.
30. Starikov, A.G., Minyaev, R.M., and Minkin, V.I., *Mendeleev Commun.*, 2009, vol. 19, p. 64.

Translated by E. Yablonskaya